IEEE Access
Multidisciplinary : Rapid Review : Open Access Journal

Received November 26, 2019, accepted December 23, 2019, date of publication December 25, 2019, date of current version January 6, 2020.

Digital Object Identifier 10.1109/ACCESS.2019.2962331

Error Analysis of NOMA-Based VLC Systems With Higher Order Modulation Schemes

ESAM M. ALMOHIMMAH AND MOHAMMED T. ALRESHEEDI
Department of Electrical Engineering, King Saud University, Riyadh 11421, Saudi Arabia

Corresponding author: Esam M. Almohimmah (ealmohimmah@ksu.edu.sa)

This work was supported by the Deanship of Scientific Research at King Saud University through the initiative of DSR Graduate Students Research Support (GSR).

ABSTRACT Nonorthogonal multiple access (NOMA) is a technique with high spectral efficiency that is expected to be applied in future wireless networks. However, its high spectral efficiency comes at the expense of increased error in data detection. This paper presents theoretical error analysis of a downlink power-domain NOMA-based visible light communication (VLC) system with higher order modulation schemes in which the scenario of imperfect successive interference cancellation (SIC) is considered. Exact closed-form expressions for the symbol error rates (SERs) of the users are derived when the modulation is the square quadrature amplitude modulation (QAM). The derived expressions are applicable to any modulation order of each user. In addition, a necessary and sufficient power allocation (PA) constraint is provided for NOMA with higher order modulation to ensure that the decision regions of the symbols in the superimposed constellation do not intersect or overlap. The simulation results support the theoretical analysis and the accuracy of the derived expressions. The results demonstrate that the user SER in NOMA-based systems can be minimized with a suitable PA that depends on the modulation orders of the users.

INDEX TERMS Nonorthogonal multiple access (NOMA), visible light communication (VLC), symbol error rate, successive interference cancellation (SIC), power allocation.

I. INTRODUCTION

Future wireless networks will require high spectral efficiency, high throughput, and massive connectivity to keep up with the tremendous growth of the demand for wireless data transmission. These requirements are becoming difficult to satisfy using the current radio frequency (RF) band as it becomes increasingly saturated [1]. Recently, visible light communication (VLC) has been considered as an efficient alternative to indoor wireless communication due to its wider bandwidth, which does not interfere with the RF spectrum; its ability to provide ubiquitous connectivity; and its energy efficiency [2].

The requirements that are specified above for future wireless networks can be satisfied by VLC if an efficient multiple-access scheme is utilized [3]. One of the most promising multiple-access schemes, which was recently proposed, is nonorthogonal multiple access (NOMA), which is characterized by high spectral efficiency. In NOMA, multiple users can share the same time/frequency resource block; hence, massive connectivity and high throughput can be realized. NOMA employs multi-user superposition transmission (MUST) at the transmitter and a multi-user detection (MUD), such as successive interference cancellation (SIC), at the receiver [4].

Many studies have been reported in the literature on the application of NOMA technology in VLC. According to [5], [6], NOMA is suitable for downlink VLC systems for several reasons: First, a VLC cell can support a small number of users, which limits the inter-user interference in NOMA. Second, the estimation of the channel in VLC systems is easier since the channel remains constant most of the time. Thus, NOMA can use the channel state information to implement the power allocation at the transmitter and the interference cancellation at the receiver.

To further increase the spectral efficiency of NOMA-based VLC systems, higher order modulation schemes, such as quadrature amplitude modulation (QAM), can be used. Since indoor VLC is based on intensity modulation/direct detection (IM/DD) [7], QAM cannot be directly implemented for VLC because it results in complex-valued and bipolar

The associate editor coordinating the review of this manuscript and approving it for publication was Syed Mohammad Zafaruddin.

symbols. To overcome this issue, we can use one of the optical orthogonal frequency division multiplexing (O-OFDM) techniques through which a real-valued time-domain signal can be obtained by using the concept of Hermitian symmetry [8]. Then, a unipolar time-domain signal can be obtained by adding a positive direct current (DC) to the OFDM signal, such as in the direct-current O-OFDM (DCO-OFDM), or by enabling transmission on odd subcarriers only, such as in asymmetrically clipped O-OFDM (ACO-OFDM) [9].

The realization of massive connectivity and high spectral efficiency in NOMA systems comes at the expense of increased error in data detection due to the inevitable inter-user interference [10]. Without careful power allocation (PA), the use of NOMA with higher order modulation could increase the effects of the inter-user interference on the transmitted signal. In this paper, we identify a necessary and sufficient PA constraint for the feasibility of NOMA when higher order modulation is used.

Although NOMA has been extensively explored in the literature, most NOMA-based VLC studies consider lower order modulation schemes and assume perfect SIC. Therefore, the error performance of NOMA-based VLC systems with higher order modulation remains an open issue that must be carefully addressed.

A. RELATED WORK

Many studies have been reported in the literature on the application of NOMA technology in VLC. The NOMA-based VLC was proposed in [5], where the authors proposed the gain ratio power allocation (GRPA) method. In [11], Haas et al. found that NOMA can always increase the throughput of LiFi (light-fidelity, which is a fully networked VLC system) networks. They also found that NOMA can improve the performance of attocell edge users without significantly affecting the performance of other users. In [12], the authors proposed a normalized gain difference power allocation (NGDPA) method for a 2 $\times$ 2 MIMO-NOMA-based VLC system and demonstrated that it outperforms GRPA in terms of the system sum-rate. Enhanced PA for OFDM-NOMA-based VLC with an arbitrary number of multiplexed users has been proposed in [13]. Power optimization has been performed at both the user level and the subcarrier level. The results demonstrated an enhancement in the system sum-rate compared to the GRPA algorithm. The authors in [14], [15] derived closed-form expressions of the system coverage probability and the ergodic sum rate. The probability that the individual rates are higher in NOMA than in OMA has also been derived.

To avoid the SIC process and to improve the performance of the NOMA-based VLC system with M-QAM, the authors in [16] proposed an algorithm for data detection: the ergodicity and comparison (EAC) algorithm. In [17], a flexible-rate SIC-free NOMA technique for downlink VLC systems has been proposed that uses the concepts of constellation partitioning coding (CPC) and uneven constellation demapping (UCD). The effect of the error propagation that results from imperfect SIC can be efficiently mitigated. In [18], the authors proposed symmetric superposition coding (SSC) and symmetric SIC (SSIC) decoding for a NOMA-based VLC system. Using SSC and SSIC, some of the second-user adjacent decision regions will have the same symbol. Hence, the effect of the error propagation is mitigated. Although this study showed enhancement of the performance of the system, it did not identify the PA that guarantees the best performance.

A closed-form expression for the bit error rate (BER) of a single-light-emitting diode (LED) downlink NOMA-based VLC system with on-off keying (OOK) has been derived under perfect channel state information (CSI) in [19], [20]. Moreover, a simple and accurate approximation for the upper bound under noisy and outdated CSI has been derived. In [21], the authors derived a mathematical expression for the SER of a multi-LED downlink NOMA-based VLC system. The authors in [22] derived BER expressions for NOMA-based VLC with M-ary phase shift keying (PSK) that are based on a bitwise-decision axis and signal space. The derived expressions hold for any modulation order.

In [23], the pairwise error probability (PEP) of NOMA systems was investigated over Nakagami-*m* fading channels. PEP expressions are derived and used to derive an exact union bound on the bit error rate (BER). In [24], the BER performance of downlink NOMA systems over Nakagami-*m* fading channels was investigated. They considered two scenarios: 2-user NOMA and 3-user NOMA. In both [23] and [24], the derived BER expressions are for the quadrature phase-shift keying (QPSK) scheme. In contrast to [23] and [24], this paper investigates the performance of downlink NOMA-based VLC systems with higher order modulation schemes. A more general scenario is considered, in which the users' signals are generated by square M-QAM. The derivation of the user SER is straightforward and is applicable to any M_1 and M_2 values. Furthermore, the analysis that is introduced in this paper can be extended to other NOMA-based communication systems.

B. CONTRIBUTIONS

In this paper, we provide an error analysis for NOMA-based VLC systems with higher order modulation. The imperfect SIC case has been considered and computer simulations have been conducted to evaluate the accuracy of the theoretical analysis. The main contributions of this paper are summarized as follows:

- *SER Analysis*: We derived exact closed-form expressions for the user SER in a two-user NOMA-based VLC system if the symbols of each user are generated using any square M-QAM. The imperfect SIC case has been considered.
- *PA constraint*: We demonstrated how improper PA could cause the users' symbols to overlap in the superimposed constellation, which will render the symbols indistinguishable. We derived a general mathematical formula for calculating the value of the PA coefficient that causes the overlap in the superimposed constellation. Based on

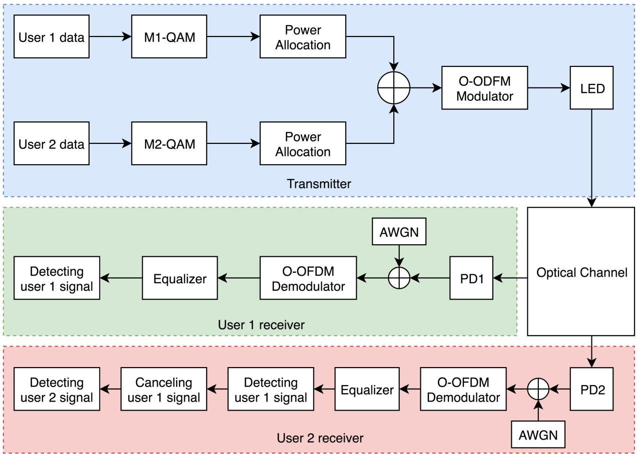

FIGURE 1. Block diagram for a 2-user NOMA-based VLC system with QAM and O-OFDM.

that, we provided a necessary and sufficient PA constraint in higher order modulation NOMA for ensuring that the symbols of the users do not overlap in the superimposed constellation.

- *Optimal PA*: We derived a mathematical formula for identifying the optimal PA, namely, the PA that minimizes the SER of the second user, which is the strong user. The derived PA represents the optimal trade-off between reducing the interference to decode the first-user signal and reducing the effect of the noise to decode the second-user signal.
- *Modulation Order Effect*: We explain how the modulation order of each user plays an important role in determining the PA that ensures the quality of service that is required for both users. We also demonstrate how the optimal PA changes according to the modulation order of each user.

C. PAPER ORGANIZATION

The remainder of this paper is organized as follows: In Section II, the system model of NOMA-based VLC with higher order modulation is described. In Section III, the user SER of square M-QAM in NOMA-based VLC systems is derived. Section IV proposes a PA constraint for higher order modulation NOMA-based VLC. The results are presented and discussed in Section V. Finally, Section VI presents the conclusions of this paper.

II. SYSTEM MODEL

Fig. 1 presents a block diagram of a downlink 2-user NOMA-based VLC system with a single LED. M_k-QAM is used to map the user data, where $k \in \{1, 2\}$. Power is allocated to the signal of each user. Then, the signals are combined. The superimposed signal is modulated by O-OFDM. Although we can use any O-OFDM, in this paper, we use ACO-OFDM to avoid the introduction of additional noise due to the clipping of the negative values in DCO-OFDM or any O-OFDM with DC bias. Then, the LED converts the electrical signal into an optical signal. At the receiver, the first user will directly decode its signal from the received signal while regarding the second-user signal as noise. In addition, the second user will perform SIC to decode its signal.

Fig. 2 presents an example of the constellation of the superimposed symbols when the first-user symbols are generated by 4-QAM with an average power of p_1 and the second-user symbols are generated by 16-QAM with an average power of p_2. In the superimposed constellation, the constellation of the second user is replicated for each symbol of the first user. Each replica represents one symbol for the first user. Hence, the constellation of the superimposed symbols consists of $M_x = M_1 \times M_2$ symbols.

In our analysis, we consider the special case of a rectangular QAM, which is called the square QAM. In the square QAM, the number of bits per symbol is an even number, or, simply, the modulation order is 4^q, where $q \in \{1, 2, \cdots\}$. In the square M-QAM constellation, the in-phase and quadrature alphabets are expressed as follows [25]:

$$A_I = \{\pm (2m - 1)\} \tag{1a}$$
$$A_Q = \{\pm (2n - 1)\} \tag{1b}$$

where $m, n \in \left\{1, 2, \cdots, \sqrt{M}/2\right\}$. The average energy is expressed as follows [26]:

$$E_{avg} = \frac{2}{3}(M - 1) \tag{2}$$

Let s_1 and s_2 be the symbols of the first and second users, respectively. Let a_1 and a_2 be the PA coefficients of the two users. Then, s_1 is expressed as:

$$s_1 = A_{I1}\xi_1\sqrt{a_1 E_s} + jA_{Q1}\xi_1\sqrt{a_1 E_s} \tag{3}$$

where A_{I1} and $A_{Q1} \in \left\{\pm 1, \pm 3, \cdots, \pm\left(\sqrt{M_1} - 1\right)\right\}$ are the in-phase and quadrature alphabets, respectively; $\xi_1 = \left(\frac{2}{3}(M_1 - 1)\right)^{-1}$ is a normalization factor; and E_s is the total average energy. Similarly, s_2 is expressed as:

$$s_2 = A_{I2}\xi_2\sqrt{a_2 E_s} + jA_{Q2}\xi_2\sqrt{a_2 E_s} \tag{4}$$

where A_{I2} and $A_{Q2} \in \left\{\pm 1, \pm 3, \cdots, \pm\left(\sqrt{M_2} - 1\right)\right\}$ and $\xi_2 = \left(\frac{2}{3}(M_2 - 1)\right)^{-1}$. The superimposed symbol is expressed as follows:

$$\begin{aligned} x &= \sqrt{E_s}\left(A_{I1}\xi_1\sqrt{a_1} + A_{I2}\xi_2\sqrt{a_2}\right) \\ &\quad + j\sqrt{E_s}\left(A_{Q1}\xi_1\sqrt{a_1} + A_{Q2}\xi_2\sqrt{a_2}\right) \\ &= A_{Ix} + jA_{Qx} \end{aligned} \tag{5}$$

where $A_{Ix} = \sqrt{E_s}\left(A_{I1}\xi_1\sqrt{a_1} + A_{I2}\xi_2\sqrt{a_2}\right)$ and $A_{Qx} = \sqrt{E_s}\left(A_{Q1}\xi_1\sqrt{a_1} + A_{Q2}\xi_2\sqrt{a_2}\right)$. The received signal at user k is expressed as:

$$y_k = g_k x + n_k \tag{6}$$

where $k \in \{1, 2\}$; $g_k = \eta\mathcal{R}_k h_k$ is the total channel gain for user k; η is the electrical-to-optical efficiency of the LED,

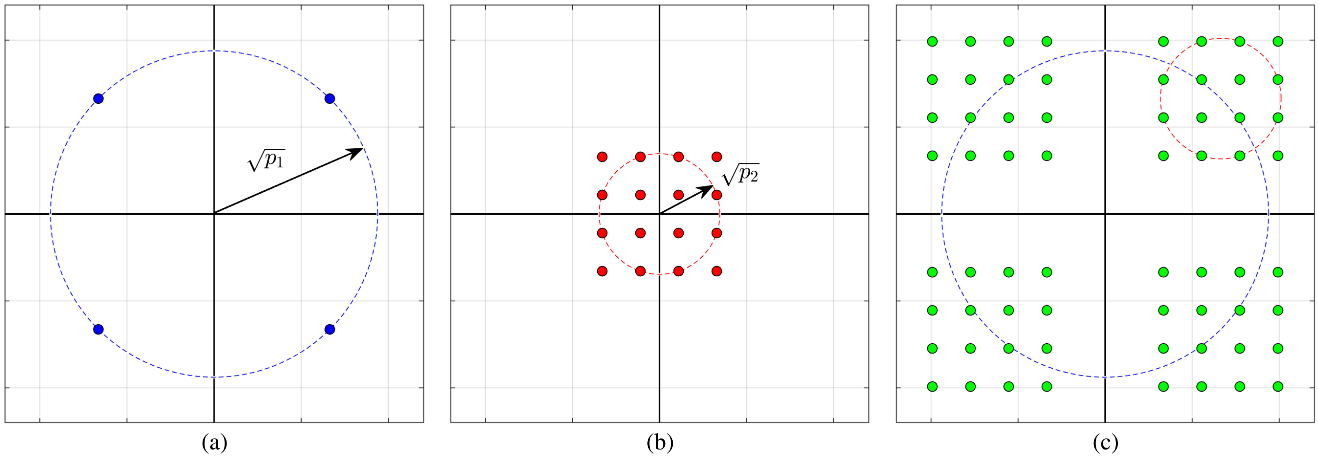

FIGURE 2. Constellations of (a) first-user symbols, (b) second-user symbols, and (c) superimposed symbols.

$\mathcal{R}_k$ is the responsivity of the photodetector (PD), and h_k is the optical channel gain, which is expressed as follows [15]:

$$h_k = \frac{(m+1)A_k T(\psi_k)\, g(\psi_k)}{2\pi d_k^2} \cos^m(\phi_k)\cos(\psi_k) \quad (7)$$

where $m = -1/\log_2\left(\cos\left(\Phi_{1/2}\right)\right)$ is the order of the Lambertian emission; A_k is the effective area of the PD of the user; $T(\psi_k)$ is the optical filter gain; and $g(\psi_k) = r^2/\sin^2(\Psi_k)$ is the gain of the optical concentrator with a refractive index r. The noise n_k follows the following Gaussian probability distribution function:

$$p(n) = \frac{1}{\sqrt{2\pi\sigma^2}} \exp\left(\frac{-(n-\mu)^2}{2\sigma^2}\right) \quad (8)$$

where μ and σ^2 are the mean and the variance, respectively. Here, we assume $\mu = 0$ and $\sigma^2 = N_0/2$, and we assume that g_k is known at the receiver. Hence, the received symbol after equalization is:

$$\tilde{y}_k = x + \tilde{n}_k \quad (9)$$

where $\tilde{n}_k = n_k/g_k$ is the additive Gaussian noise that is scaled by the total channel gain. To simplify the notation, we let y_k denote the equalized received symbol in the remainder of this analysis.

In the square QAM, there are three types of constellation symbols (points); corner symbols, edge symbols, and interior symbols. Let N_c, N_e, and N_i denote the numbers of corner symbols, edge symbols, and interior symbols, respectively. For any square QAM, $N_c = 4$, $N_e = 4(\sqrt{M} - 2)$, and $N_i = (\sqrt{M} - 2)^2$.

III. SER ANALYSIS

In this section, we will determine the user SER when $M_1 = 16$ and $M_2 = 16$, and we will generalize the result for any M_1 and M_2. When both users have a 16-QAM constellation, the superimposed signal will have a constellation with 256 symbols.

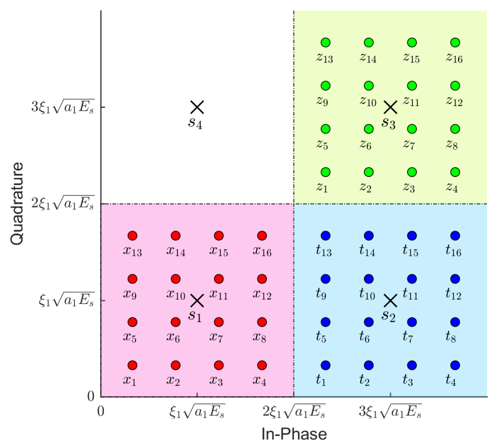

FIGURE 3. First quadrant of the superimposed signal constellation, which shows the decision regions for the interior symbol s_1, the edge symbol s_2, and the corner symbol s_3.

A. SER FOR THE FIRST USER

To determine the SER for the first user, we must calculate the error probability in the detection of the first-user symbol for each symbol type. Fig. 3 presents the decision regions for four symbols of the first user on the first quadrant of the superimposed signal constellation, in which s_1 is an interior symbol, s_2 and s_4 are edge symbols, and s_3 is a corner symbol.

1) ERROR PROBABILITY OF THE INTERIOR SYMBOLS

The error probability in the detection of an interior symbol can be calculated as follows: First, we consider the interior symbol s_1. The possible superimposed symbols that are associated with s_1 are presented in red in Fig. 3 and denoted by x_i, $i \in \{1, 2, \cdots, 16\}$. The superimposed symbol x_i is expressed as:

$$x_i = \sqrt{E_s}\left(\xi_1\sqrt{a_1} + A_{I2_i}\xi_2\sqrt{a_2}\right) + j\sqrt{E_s}\left(\xi_1\sqrt{a_1} + A_{Q2_i}\xi_2\sqrt{a_2}\right) \quad (10)$$

where A_{I2_i} and $A_{Q2_i} \in \{\pm 1, \pm 3\}$. The probability of decoding s_1 correctly given that x_i was sent can be calculated as follows:

$$\Pr\left\{c_{s_1}|x_i\right\} = \Pr\left\{c_{s_1}|x_i\right\}_I \times \Pr\left\{c_{s_1}|x_i\right\}_Q \tag{11}$$

where

$$\Pr\left\{c_{s_1}|x_i\right\}_I = \Pr\left\{0 < \Re(y_k) < 2\xi_1\sqrt{a_1\, E_s}\right\}$$

and

$$\Pr\left\{c_{s_1}|x_i\right\}_Q = \Pr\left\{0 < \Im(y_k) < 2\xi_1\sqrt{a_1\, E_s}\right\}$$

$\Re(\cdot)$ and $\Im(\cdot)$ are the real and imaginary operators, respectively.

Via (8), $\Pr\left\{c_{s_1}|x_i\right\}_I$ can be calculated as follows:

$$\begin{aligned}
\Pr\left\{c_{s_1}|x_i\right\}_I &= \frac{1}{\sqrt{\pi N_k}} \int_0^{2\xi_1\sqrt{a_1 E_s}} \exp\left(-\frac{\Re\left(y_k - x_i\right)^2}{N_k}\right) dy_k \\
&= 1 - \frac{1}{\sqrt{\pi N_k}} \left(\int_{-\infty}^{0} \exp\left(-\frac{\Re\left(y_k - x_i\right)^2}{N_k}\right) dy_k \right. \\
&\quad \left. + \int_{2\xi_1\sqrt{a_1 E_s}}^{\infty} \exp\left(-\frac{\Re\left(y_k - x_i\right)^2}{N_k}\right) dy_k \right) \\
&= 1 - Q\left(u_i\right) - Q\left(\tilde{u}_i\right)
\end{aligned} \tag{12}$$

where N_k, u_i, $\tilde{u}_i$, and $Q(\cdot)$ are expressed as:

$$\begin{aligned}
N_k &= \frac{N_0}{g_k^2} \\
u_i &= \sqrt{\frac{2}{N_k}}\Re(x_i) \\
\tilde{u}_i &= \sqrt{\frac{2}{N_k}}\left(2\xi_1\sqrt{a_1\, E_s} - \Re(x_i)\right) \\
Q(x) &= \frac{1}{\sqrt{2\pi}} \int_x^{\infty} \exp\left(-\frac{u^2}{2}\right) du
\end{aligned}$$

Similarly,

$$\Pr\left\{c_{s_1}|x_i\right\}_Q = 1 - Q\left(v_i\right) - Q\left(\tilde{v}_i\right) \tag{13}$$

where v_i and $\tilde{v}_i$ are expressed as:

$$\begin{aligned}
v_i &= \sqrt{\frac{2}{N_k}}\Im(x_i) \\
\tilde{v}_i &= \sqrt{\frac{2}{N_k}}\left(2\xi_1\sqrt{a_1 E_s} - \Im(x_i)\right)
\end{aligned} \tag{14}$$

Therefore,

$$\begin{aligned}
\Pr\left\{c_{s_1}|x_i\right\} &= \left(1 - Q\left(u_i\right) - Q\left(\tilde{u}_i\right)\right)\left(1 - Q\left(v_i\right) - Q\left(\tilde{v}_i\right)\right) \\
&= 1 - Q\left(u_i\right) - Q\left(\tilde{u}_i\right) - Q\left(v_i\right) - Q\left(\tilde{v}_i\right) \\
&\quad + Q\left(u_i\right) Q\left(v_i\right) + Q\left(\tilde{u}_i\right) Q\left(v_i\right) \\
&\quad + Q\left(u_i\right) Q\left(\tilde{v}_i\right) + Q\left(\tilde{u}_i\right) Q\left(\tilde{v}_i\right)
\end{aligned} \tag{15}$$

Now, the error probability in the decoding of s_1 given that x_i was sent can be calculated as:

$$\begin{aligned}
\Pr\left\{e_{s_1}|x_i\right\} &= 1 - \Pr\left\{c_{s_1}|x_i\right\} \\
&= Q\left(u_i\right) + Q\left(\tilde{u}_i\right) + Q\left(v_i\right) + Q\left(\tilde{v}_i\right) \\
&\quad - Q\left(u_i\right) Q\left(v_i\right) - Q\left(\tilde{u}_i\right) Q\left(v_i\right) \\
&\quad - Q\left(u_i\right) Q\left(\tilde{v}_i\right) - Q\left(\tilde{u}_i\right) Q\left(\tilde{v}_i\right)
\end{aligned} \tag{16}$$

u_i and v_i can take any of the following values:

$$\begin{aligned}
w_1 &= \gamma_k\left(\xi_1\sqrt{a_1} - 3\xi_2\sqrt{a_2}\right) \\
w_2 &= \gamma_k\left(\xi_1\sqrt{a_1} - \xi_2\sqrt{a_2}\right) \\
w_3 &= \gamma_k\left(\xi_1\sqrt{a_1} + \xi_2\sqrt{a_2}\right) \\
w_4 &= \gamma_k\left(\xi_1\sqrt{a_1} + 3\xi_2\sqrt{a_2}\right)
\end{aligned} \tag{17}$$

where $\gamma_k = \sqrt{2\, g_k^2\, E_s/N_0}$. The expression for w_i in (17) can be generalized to any M_2 as follows:

$$w_i = \gamma_k\left(\xi_1\sqrt{a_1} + A_i\xi_2\sqrt{a_2}\right) \tag{18}$$

where A_i is the alphabet of the second user constellation, which can be expressed as:

$$A_i = 2i - 1 - \sqrt{M_2} \tag{19}$$

where $i \in \left\{1, 2, \cdots, \sqrt{M_2}\right\}$. According to (17), the values of u_i and v_i satisfy the following:

$$\begin{aligned}
u_1 &= u_5 = u_9 = u_{13} = v_1 = v_2 = v_3 = v_4 = w_1 \\
u_2 &= u_6 = u_{10} = u_{14} = v_5 = v_6 = v_7 = v_8 = w_2 \\
u_3 &= u_7 = u_{11} = u_{15} = v_9 = v_{10} = v_{11} = v_{12} = w_3 \\
u_4 &= u_8 = u_{12} = u_{16} = v_{13} = v_{14} = v_{15} = v_{16} = w_4
\end{aligned} \tag{20}$$

Due to the symmetry of the constellation points x_i around s_1, the following relations hold: $u_1 = \tilde{u}_4$, $u_2 = \tilde{u}_3$, $u_3 = \tilde{u}_2$, and $u_4 = \tilde{u}_1$. Similarly, $v_1 = \tilde{v}_4$, $v_2 = \tilde{v}_3$, $v_3 = \tilde{v}_2$, and $v_4 = \tilde{v}_1$. Therefore, from (16) we obtain:

$$\begin{aligned}
\Pr\left\{e_{s_1}|x_1\right\} &= \Pr\left\{e_{s_1}|x_4\right\} = \Pr\left\{e_{s_1}|x_{13}\right\} = \Pr\left\{e_{s_1}|x_{16}\right\} \\
&= 2Q\left(w_1\right) + 2Q\left(w_4\right) - Q\left(w_1\right)^2 \\
&\quad - 2Q\left(w_1\right) Q\left(w_4\right) - Q\left(w_4\right)^2
\end{aligned} \tag{21}$$

Similarly,

$$\begin{aligned}
\Pr\left\{e_{s_1}|x_2\right\} &= \Pr\left\{e_{s_1}|x_3\right\} = \Pr\left\{e_{s_1}|x_5\right\} = \Pr\left\{e_{s_1}|x_8\right\} \\
&= \Pr\left\{e_{s_1}|x_9\right\} = \Pr\left\{e_{s_1}|x_{12}\right\} = \Pr\left\{e_{s_1}|x_{14}\right\} \\
&= \Pr\left\{e_{s_1}|x_{15}\right\} \\
&= Q\left(w_1\right) + Q\left(w_2\right) + Q\left(w_3\right) + Q\left(w_4\right) \\
&\quad - Q\left(w_1\right) Q\left(w_2\right) - Q\left(w_1\right) Q\left(w_3\right) \\
&\quad - Q\left(w_2\right) Q\left(w_4\right) - Q\left(w_3\right) Q\left(w_4\right)
\end{aligned} \tag{22}$$

and

$$\begin{aligned}
\Pr\left\{e_{s_1}|x_6\right\} &= \Pr\left\{e_{s_1}|x_7\right\} = \Pr\left\{e_{s_1}|x_{10}\right\} = \Pr\left\{e_{s_1}|x_{11}\right\} \\
&= 2Q\left(w_2\right) + 2Q\left(w_3\right) - Q\left(w_2\right)^2 \\
&\quad - 2Q\left(w_2\right) Q\left(w_3\right) - Q\left(w_3\right)^2
\end{aligned} \tag{23}$$

The probability of error in decoding s_1 can be calculated as follows:

$$\Pr\left\{e_{s_1}\right\} = \sum_{i=1}^{16} \Pr\left\{x_i\right\} \Pr\left\{e_{s_1}|x_i\right\} = \frac{1}{16}\sum_{i=1}^{16} \Pr\left\{e_{s_1}|x_i\right\} \tag{24}$$

Using (21), (22), and (23), Eq. (24) can be reformulated as:

$$\Pr\left\{e_{s_1}\right\} = \frac{1}{16}\sum_{i=1}^{4}\sum_{j=1}^{4} 4Q\left(w_i\right) - 4Q\left(w_i\right)Q\left(w_j\right) \tag{25}$$

Eq. (25) can be generalized to any M_2 as follows:

$$\Pr\left\{e_{s_1}\right\} = \frac{1}{M_2}\sum_{i=1}^{\sqrt{M_2}}\sum_{j=1}^{\sqrt{M_2}} 4Q\left(w_i\right) - 4Q\left(w_i\right)Q\left(w_j\right) \tag{26}$$

2) ERROR PROBABILITY OF THE CORNER SYMBOLS

The error probability in the detection of a corner symbol can be calculated as follows: First, we consider the corner symbol s_3. The possible superimposed symbols that are associated with s_3 are presented in green in Fig. 3 and denoted by z_i, $i \in \{1, 2, \cdots, 16\}$. The superimposed symbol z_i is expressed as:

$$z_i = \sqrt{E_s}\left(3\xi_1\sqrt{a_1} + A_{I2_i}\xi_2\sqrt{a_2}\right) + j\sqrt{E_s}\left(3\xi_1\sqrt{a_1} + A_{Q2_i}\xi_2\sqrt{a_2}\right) \tag{27}$$

The probability of decoding s_3 correctly given that z_i was sent can be calculated as follows:

$$\Pr\left\{c_{s_3}|z_i\right\} = \Pr\left\{c_{s_3}|z_i\right\}_I \times \Pr\left\{c_{s_3}|z_i\right\}_Q \tag{28}$$

where

$$\Pr\left\{c_{s_3}|z_i\right\}_I = \Pr\left\{2\xi_1\sqrt{a_1\,E_s} < \Re(y_k) < +\infty\right\}$$

and

$$\Pr\left\{c_{s_3}|z_i\right\}_Q = \Pr\left\{2\xi_1\sqrt{a_1\,E_s} < \Im(y_k) < +\infty\right\}$$

Using (8), $\Pr\left\{c_{s_3}|z_i\right\}_I$ can be calculated as follows:

$$\begin{aligned}\Pr\left\{c_{s_3}|z_i\right\}_I &= 1 - \frac{1}{\sqrt{\pi N_k}}\int_{-\infty}^{2\xi_1\sqrt{a_1 E_s}} \exp\left(-\frac{\Re\left(y_k - z_i\right)^2}{N_k}\right) dy_k \\ &= 1 - Q\left(u_i\right)\end{aligned} \tag{29}$$

where $u_i = \sqrt{2/N_k}\left(\Re(z_i) - 2\xi_1\sqrt{a_1\,E_s}\right)$. Similarly,

$$\Pr\left\{c_{s_3}|z_i\right\}_Q = 1 - Q\left(v_i\right) \tag{30}$$

where $v_i = \sqrt{2/N_k}\left(\Im(z_i) - 2\xi_1\sqrt{a_1\,E_s}\right)$. Therefore,

$$\begin{aligned}\Pr\left\{c_{s_3}|z_i\right\} &= \left(1 - Q\left(u_i\right)\right)\left(1 - Q\left(v_i\right)\right) \\ &= 1 - Q\left(u_i\right) - Q\left(v_i\right) + Q\left(u_i\right)Q\left(v_i\right)\end{aligned} \tag{31}$$

Then, the error probability in the decoding of s_3 given that z_i was sent can be calculated as:

$$\begin{aligned}\Pr\left\{e_{s_3}|z_i\right\} &= 1 - \Pr\left\{c_{s_3}|z_i\right\} \\ &= Q\left(u_i\right) + Q\left(v_i\right) - Q\left(u_i\right)Q\left(v_i\right)\end{aligned} \tag{32}$$

Therefore, the error probability in the decoding of s_3 can be calculated as follows:

$$\begin{aligned}\Pr\left\{e_{s_3}\right\} &= \sum_{i=1}^{16}\Pr\left\{z_i\right\}\Pr\left\{e_{s_3}|z_i\right\} \\ &= \frac{1}{16}\sum_{i=1}^{16}\Pr\left\{e_{s_3}|z_i\right\} \\ &= \frac{1}{16}\sum_{i=1}^{16}\Big(Q\left(u_i\right) + Q\left(v_i\right) - Q\left(u_i\right)Q\left(v_i\right)\Big)\end{aligned} \tag{33}$$

Due to the symmetry of the constellation points z_i around s_3 and using (17), we can reformulate (33) as:

$$\Pr\left\{e_{s_3}\right\} = \frac{1}{16}\sum_{i=1}^{4}\sum_{j=1}^{4} 2Q\left(w_i\right) - Q\left(w_i\right)Q\left(w_j\right) \tag{34}$$

Equation (34) can be generalized to any M_2 as follows:

$$\Pr\left\{e_{s_3}\right\} = \frac{1}{M_2}\sum_{i=1}^{\sqrt{M_2}}\sum_{j=1}^{\sqrt{M_2}} 2Q\left(w_i\right) - Q\left(w_i\right)Q\left(w_j\right) \tag{35}$$

3) ERROR PROBABILITY OF THE EDGE SYMBOLS

The error probability in the detection of an edge symbol can be calculated as follows: First, we consider the edge symbol s_2. The possible superimposed symbols that are associated with s_2 are presented in blue in Fig. 3 and denoted by t_i, $i \in \{1, 2, \cdots, 16\}$. The superimposed symbol t_i is expressed as:

$$t_i = \sqrt{E_s}\left(3\xi_1\sqrt{a_1} + A_{I2_i}\xi_2\sqrt{a_2}\right) + j\sqrt{E_s}\left(\xi_1\sqrt{a_1} + A_{Q2_i}\xi_2\sqrt{a_2}\right) \tag{36}$$

The probability of decoding s_2 correctly given that t_i was sent can be calculated by:

$$\Pr\left\{c_{s_2}|t_i\right\} = \Pr\left\{c_{s_2}|t_i\right\}_I \times \Pr\left\{c_{s_2}|t_i\right\}_Q \tag{37}$$

where

$$\Pr\left\{c_{s_2}|t_i\right\}_I = \Pr\left\{2\xi_1\sqrt{a_1\,E_s} < \Re(y_k) < +\infty\right\}$$

and

$$\Pr\left\{c_{s_2}|t_i\right\}_Q = \Pr\left\{0 < \Im(y_k) < 2\xi_1\sqrt{a_1\,E_s}\right\}$$

$\Pr\left\{c_{s_2}|t_i\right\}_I$ and $\Pr\left\{c_{s_2}|t_i\right\}_Q$ can be calculated similarly to $\Pr\left\{c_{s_3}|z_i\right\}_I$ and $\Pr\left\{c_{s_1}|x_i\right\}_Q$, respectively. Therefore,

$$\begin{aligned}\Pr\left\{c_{s_2}|t_i\right\} &= \left(1 - Q\left(u_i\right)\right)\left(1 - Q\left(v_i\right) - Q\left(\tilde{v}_i\right)\right) \\ &= 1 - Q\left(u_i\right) - Q\left(v_i\right) - Q\left(\tilde{v}_i\right) \\ &\quad + Q\left(u_i\right)Q\left(v_i\right) + Q\left(u_i\right)Q\left(\tilde{v}_i\right)\end{aligned} \tag{38}$$

The error probability in the decoding of s_2 given that t_i was sent can be calculated as:

$$\begin{aligned}\Pr\left\{e_{s_2}|t_i\right\} &= 1-\Pr\left\{c_{s_2}|t_i\right\}\\ &= Q(u_i)+Q(v_i)+Q(\tilde{v}_i)-Q(u_i)Q(v_i)\\ &\quad -Q(u_i)Q(\tilde{v}_i)\end{aligned}\tag{39}$$

Due to the symmetry of the constellation points t_i around s_2 and using (17), we can reformulate (39) for each t_i as follows:

$$\begin{aligned}\Pr\left\{e_{s_2}|t_1\right\} &= \Pr\left\{e_{s_2}|t_{13}\right\}\\ &= Q(w_1)+Q(w_1)+Q(w_4)\\ &\quad -Q(w_1)Q(w_1)-Q(w_1)Q(w_4)\end{aligned}\tag{40}$$

$$\begin{aligned}\Pr\left\{e_{s_2}|t_2\right\} &= \Pr\left\{e_{s_2}|t_{14}\right\}\\ &= Q(w_1)+Q(w_2)+Q(w_4)\\ &\quad -Q(w_1)Q(w_2)-Q(w_2)Q(w_4)\end{aligned}\tag{41}$$

$$\begin{aligned}\Pr\left\{e_{s_2}|t_3\right\} &= \Pr\left\{e_{s_2}|t_{15}\right\}\\ &= Q(w_1)+Q(w_3)+Q(w_4)\\ &\quad -Q(w_1)Q(w_3)-Q(w_3)Q(w_4)\end{aligned}\tag{42}$$

$$\begin{aligned}\Pr\left\{e_{s_2}|t_4\right\} &= \Pr\left\{e_{s_2}|t_{16}\right\}\\ &= Q(w_1)+Q(w_4)+Q(w_4)\\ &\quad -Q(w_1)Q(w_4)-Q(w_4)Q(w_4)\end{aligned}\tag{43}$$

$$\begin{aligned}\Pr\left\{e_{s_2}|t_5\right\} &= \Pr\left\{e_{s_2}|t_9\right\}\\ &= Q(w_1)+Q(w_2)+Q(w_3)\\ &\quad -Q(w_1)Q(w_2)-Q(w_1)Q(w_3)\end{aligned}\tag{44}$$

$$\begin{aligned}\Pr\left\{e_{s_2}|t_6\right\} &= \Pr\left\{e_{s_2}|t_{10}\right\}\\ &= Q(w_2)+Q(w_2)+Q(w_3)\\ &\quad -Q(w_2)Q(w_2)-Q(w_2)Q(w_3)\end{aligned}\tag{45}$$

$$\begin{aligned}\Pr\left\{e_{s_2}|t_7\right\} &= \Pr\left\{e_{s_2}|t_{11}\right\}\\ &= Q(w_2)+Q(w_3)+Q(w_3)\\ &\quad -Q(w_2)Q(w_3)-Q(w_3)Q(w_3)\end{aligned}\tag{46}$$

$$\begin{aligned}\Pr\left\{e_{s_2}|t_8\right\} &= \Pr\left\{e_{s_2}|t_{12}\right\}\\ &= Q(w_2)+Q(w_3)+Q(w_4)\\ &\quad -Q(w_2)Q(w_4)-Q(w_3)Q(w_4)\end{aligned}\tag{47}$$

Hence, the error probability in the decoding of s_2 can be calculated by:

$$\begin{aligned}\Pr\left\{e_{s_2}\right\} &= \sum_{i=1}^{16}\Pr\{t_i\}\Pr\left\{e_{s_2}|t_i\right\} = \frac{1}{16}\sum_{i=1}^{16}\Pr\left\{e_{s_2}|t_i\right\}\\ &= \frac{2}{16}\sum_{i=1}^{8}\Pr\left\{e_{s_2}|t_i\right\}\end{aligned}\tag{48}$$

Substituting (40) - (47) into (48) yields:

$$\begin{aligned}\Pr\left\{e_{s_2}\right\} = \frac{2}{16}\Big(&6Q(w_1)+6Q(w_2)+6Q(w_3)+6Q(w_4)\\ &-Q(w_1)^2-Q(w_2)^2-Q(w_3)^2-Q(w_4)^2\\ &-2Q(w_1)Q(w_2)-2Q(w_1)Q(w_3)\\ &-2Q(w_1)Q(w_4)-2Q(w_2)Q(w_3)\\ &-2Q(w_2)Q(w_4)-2Q(w_3)Q(w_4)\Big)\end{aligned}\tag{49}$$

Therefore, the error probability in the decoding of s_2 can be calculated by:

$$\Pr\left\{e_{s_2}\right\} = \frac{1}{16}\sum_{i=1}^{4}\sum_{j=1}^{4}3Q(w_i)-2Q(w_i)Q(w_j)\tag{50}$$

Equation (50) can be generalized to any M_2 as follows:

$$\Pr\left\{e_{s_2}\right\} = \frac{1}{M_2}\sum_{i=1}^{\sqrt{M_2}}\sum_{j=1}^{\sqrt{M_2}}3Q(w_i)-2Q(w_i)Q(w_j)\tag{51}$$

Finally, the SER for the first user can be calculated by:

$$\begin{aligned}SER_1 &= \frac{1}{M_1}\Big(N_i\Pr\left\{e_{s_1}\right\}+N_e\Pr\left\{e_{s_2}\right\}+N_c\Pr\left\{e_{s_3}\right\}\Big)\\ &= \frac{1}{M_1}\Big(\left(\sqrt{M_1}-2\right)^2\Pr\left\{e_{s_1}\right\}+4\Pr\left\{e_{s_3}\right\}\\ &\quad +4\left(\sqrt{M_1}-2\right)\Pr\left\{e_{s_2}\right\}\Big)\end{aligned}\tag{52}$$

Substituting (26), (35), and (51) into (52) yields an expression for SER_1, which is presented as (53), shown at the bottom of the next page. For high SNR values, the second term in the right-hand side of (53) becomes negligible. Therefore, (53) can be approximated as:

$$SER_1 \approx \frac{4\left(\sqrt{M_1}-1\right)}{\sqrt{M_1M_2}}\sum_{i=1}^{\sqrt{M_2}}Q\big(\gamma_1\left(\xi_1\sqrt{a_1}+A_i\xi_2\sqrt{a_2}\right)\big)\tag{54}$$

B. SER FOR THE SECOND USER

The SER for the second user can be calculated by:

$$SER_2 = (1-SER_{2\to1})\,SER_{2\to2}+SER_{2\to1}\tag{55}$$

where $SER_{2\to1}$ is the SER for the second user for the detection of the first-user signal and $SER_{2\to2}$ is the SER for the second user for the detection of its own signal after detecting and canceling the first-user signal successfully. $SER_{2\to1}$ can be calculated via (56), which is presented at the top of the next page and can be obtained by replacing γ_1 in (53) with γ_2. $SER_{2\to2}$ can be calculated by replacing a_2 and M_2 in (56), as shown at the bottom of the next page, with 0 and 1, respectively. Then, we change the variables M_1, ξ_1, and a_1 to M_2, ξ_2, and a_2, respectively. Therefore, $SER_{2\to2}$ can be calculated via (57), as shown at the bottom of the next page. Finally, SER_2 can be calculated by substituting (56) and (57) into (55). For high SNR values, the second term in the right-hand side of (57) becomes negligible. Therefore, (57) can be approximated by:

$$SER_{2\to2} \approx 4\left(1-\frac{1}{\sqrt{M_2}}\right)Q\left(\gamma_2\xi_2\sqrt{a_2}\right)\tag{58}$$

IV. PA CONSTRAINT

Most NOMA studies rely on the following PA constraint to ensure the successful decoding of users' signals:

$$h_1 < h_2 < \cdots < h_K \Rightarrow p_1 > p_2 > \cdots > p_K\tag{59}$$

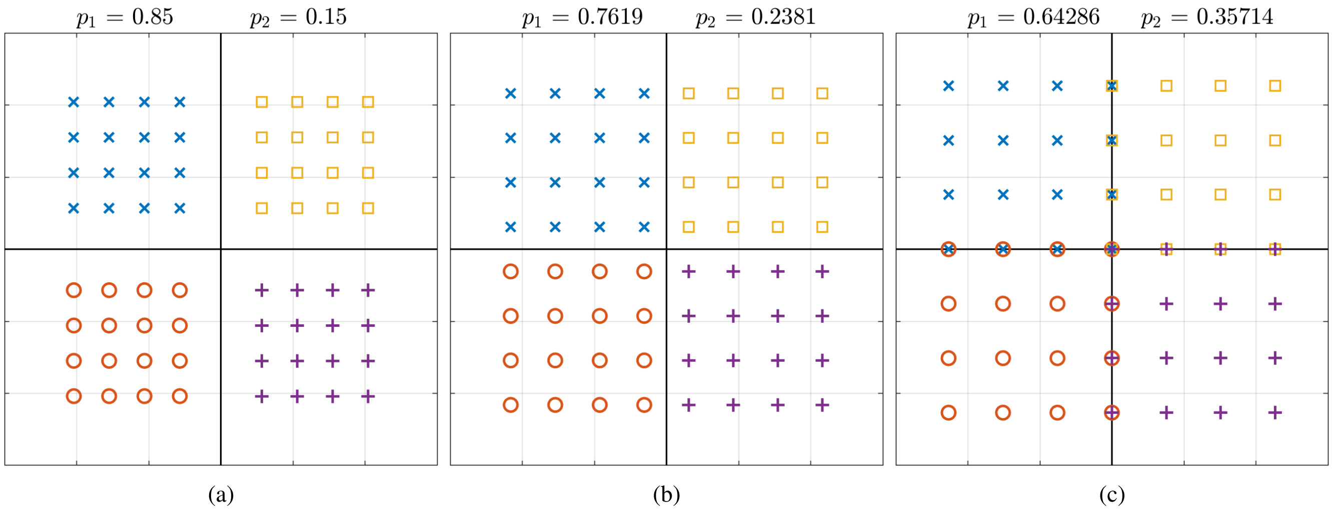

FIGURE 4. Superimposed constellations with various PAs. The horizontal and vertical axes are the in-phase and quadrature axes, respectively.

Although the condition in (59) is necessary, it is not sufficient. That is because the symbols in the superimposed constellation may overlap even if this condition is satisfied, especially when higher modulation orders are used. Hence, in a 2-user scenario, the power of the second user should not exceed a limit to ensure that the decision regions of the superimposed symbols do not overlap. This limit depends on the modulation order for each user, as we will show shortly.

Fig. 4 presents three scenarios of the superimposed constellation when 4-QAM is used for first user and 16-QAM for the second user. In each scenario, various power values are allocated to the users. Fig. 4a presents the superimposed constellation when $p_2 = 0.15$. In this case, the replicas of the second-user constellation are far apart from each other; hence, it is easier to decode the first-user symbols. When $p_2 = 0.238$, as presented in Fig. 4b, the symbols in the superimposed constellation are all equidistant, and the superimposed constellation is similar to the standard QAM constellation with $M = M_1 \times M_2$. When $p_2 = 0.357$, as presented in Fig. 4c, the minimum distance of the second user symbols is increased. However, some of the symbols in the superimposed constellation start to overlap. In this case, it is difficult to correctly decode the first-user symbols. Although $p_1 > p_2$ in the last scenario, some symbols in the superimposed constellation have overlapped. Therefore, the condition $p_1 > p_2$ is necessary but not sufficient for ensuring successful decoding.

$$
\begin{aligned}
SER_1 &= \frac{4}{M_1 M_2} \sum_{i=1}^{\sqrt{M_2}} \sum_{j=1}^{\sqrt{M_2}} \left(\left(M_1 - \sqrt{M_1} \right) Q\left(w_i\right) - \left(M_1 - 2\sqrt{M_1} + 1 \right) Q\left(w_i\right) Q\left(w_j\right) \right) \\
&= \frac{4}{M_1 M_2} \sum_{i=1}^{\sqrt{M_2}} \sum_{j=1}^{\sqrt{M_2}} \left(\left(M_1 - \sqrt{M_1} \right) Q\big(\gamma_1 \left(\xi_1 \sqrt{a_1} + A_i \xi_2 \sqrt{a_2}\right)\big) \right. \\
&\quad \left. - \left(M_1 - 2\sqrt{M_1} + 1 \right) Q\big(\gamma_1 \left(\xi_1 \sqrt{a_1} + A_i \xi_2 \sqrt{a_2}\right)\big) \times Q\big(\gamma_1 \left(\xi_1 \sqrt{a_1} + A_j \xi_2 \sqrt{a_2}\right)\big) \right) \qquad (53)
\end{aligned}
$$

$$
\begin{aligned}
SER_{2\to 1} &= \frac{4}{M_1 M_2} \sum_{i=1}^{\sqrt{M_2}} \sum_{j=1}^{\sqrt{M_2}} \left(\left(M_1 - \sqrt{M_1} \right) Q\big(\gamma_2 \left(\xi_1 \sqrt{a_1} + A_i \xi_2 \sqrt{a_2}\right)\big) \right. \\
&\quad \left. - \left(M_1 - 2\sqrt{M_1} + 1 \right) Q\big(\gamma_2 \left(\xi_1 \sqrt{a_1} + A_i \xi_2 \sqrt{a_2}\right)\big) \times Q\big(\gamma_2 \left(\xi_1 \sqrt{a_1} + A_j \xi_2 \sqrt{a_2}\right)\big) \right) \qquad (56)
\end{aligned}
$$

$$
SER_{2\to 2} = 4\left(1 - \frac{1}{\sqrt{M_2}}\right) Q\left(\gamma_2 \xi_2 \sqrt{a_2}\right) - 4\left(1 - \frac{2}{\sqrt{M_2}} + \frac{1}{M_2}\right) Q\left(\gamma_2 \xi_2 \sqrt{a_2}\right)^2 \qquad (57)
$$

A. MINIMUM PA FOR THE FIRST USER

To guarantee that the decision regions of the first-user symbols do not overlap, namely, that the points in the superimposed constellation do not cross the in-phase and quadrature axes, the following condition should be satisfied:

$$\sqrt{a_1\xi_1E_s}+A_{2min}\sqrt{a_2\xi_2E_s}>0 \tag{60}$$

where $A_{2min}=-\left(\sqrt{M_2}-1\right)$. This condition ensures that the sum of the first-user symbol with alphabet $A_1=1$ and the second-user symbol with alphabet $A_2=A_{2min}$ is greater than zero. The first overlap in the superimposed constellation occurs when the symbol with the smallest real value and the symbol with the largest real value in two adjacent replicas are equal. Therefore,

$$\sqrt{a_1\xi_1E_s}+A_{2min}\sqrt{a_2\xi_2E_s}=-\sqrt{a_1\xi_1E_s}+A_{2max}\sqrt{a_2\xi_2E_s} \tag{61}$$

where $A_{2max}=\left(\sqrt{M_2}-1\right)$. Hence,

$$\begin{aligned} a_1\xi_1 &= A_{2max}^2a_2\xi_2 \\ a_1 &= \frac{(M_1-1)\left(\sqrt{M_2}-1\right)}{2+M_1\sqrt{M_2}-M_1} \end{aligned} \tag{62}$$

Similarly, the second overlap occurs when

$$\sqrt{a_1\xi_1E_s}+A_{2min}\sqrt{a_2\xi_2E_s}= -\sqrt{a_1\xi_1E_s}+(A_{2max}-2)\sqrt{a_2\xi_2E_s} \tag{63}$$

and the n^{th} overlap occurs when

$$a_1=\frac{(M_1-1)\left(\sqrt{M_2}-n\right)^2}{(M_2-1)+(M_1-1)\left(\sqrt{M_2}-n\right)^2} \tag{64}$$

Thus, to avoid symbol overlap, the PA coefficient of the first user should be larger than the value that causes the first overlap.

B. OPTIMAL PA FOR THE SECOND USER

As the PA coefficient of the second user decreases, the minimum distance for the symbols of the second-user constellation decreases and the effect of the AWGN increases. In contrast, as the PA coefficient of the second user increases, the minimum distance increases, but the effect of the interference from the first user increases. Hence, the optimal PA for the second user is the PA that represents the best trade-off between reducing the interference for the decoding of the first-user signal and reducing the effect of the noise for the decoding of the second-user signal. Therefore, the optimal PA for the second user is the PA with which all symbols in the superimposed constellation equidistant, namely, the optimal PA for the second user is the PA that makes the superimposed constellation similar to the standard square QAM constellation with $M=M_1\times M_2$.

The minimum distance between the symbols in the square QAM constellation is expressed as [25]:

$$d_{min}^2=\frac{6}{M-1}E_{avg} \tag{65}$$

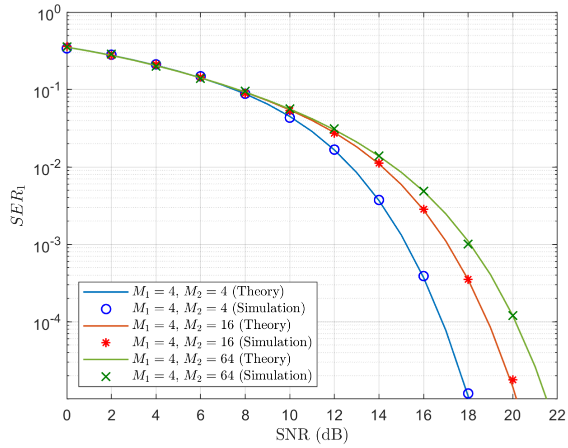

FIGURE 5. SER of the first user with $a_1=0.85$, $M_1=4$, and $M_2=4$, 16, and 64.

If we want the superimposed constellation to be similar to the constellation of the square $(M_1\times M_2)$-QAM, the minimum distance of the second-user constellation and the minimum distance of the superimposed constellation should be equal. Therefore,

$$d_{x_{min}}^2=d_{2_{min}}^2 \tag{66}$$

From (65) and (66), we obtain:

$$\frac{E_x}{M_1M_2-1}=\frac{E_2}{M_2-1} \tag{67}$$

Since $E_2=a_2\,E_x$ and $a_1+a_2=1$, the optimal PA for the second user is:

$$a_1=\frac{M_1M_2-M_2}{M_1M_2-1} \tag{68a}$$

$$a_2=\frac{M_2-1}{M_1M_2-1} \tag{68b}$$

V. RESULTS AND DISCUSSIONS

In this section, the numerical and simulation results are presented for various modulation orders.

The theoretical and simulated SERs of the first and second users are plotted in Figs. 5 and 6, respectively, with $M_1=4$ and $M_2=4$, 16, and 64. The PA coefficients are $a_1=0.85$ and $a_2=0.15$. According to Figs. 5 and 6, the simulation results perfectly match the theoretical results, which supports our analysis and the validity of the derived SER expressions.

Figs. 7 and 8 show how SER_1 and SER_2 vary with the PA coefficient a_1 for various SNR values when $M_1=4$ and $M_2=16$. SER_1 decreases as the value of a_1 increases, which is expected in this case because the interference from the second user is reduced as a_1 increases. However, SER_2 begins to decrease to its minimum value as the PA coefficient a_1 increases and subsequently starts to increase again. SER_2 initially decreases because the interference is reduced as a_1 increases; hence, the second user can more accurately cancel out the interference from the first user during the SIC process. However, as a_1 increases further, the power that is allocated

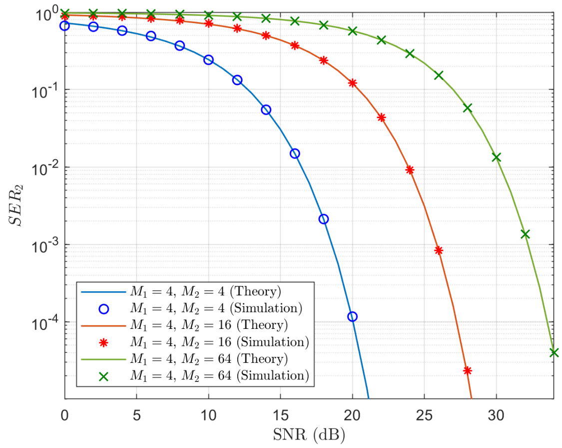

FIGURE 6. SER of the second user with $a_1 = 0.85$, $M_1 = 4$, and $M_2 = 4$, 16, and 64.

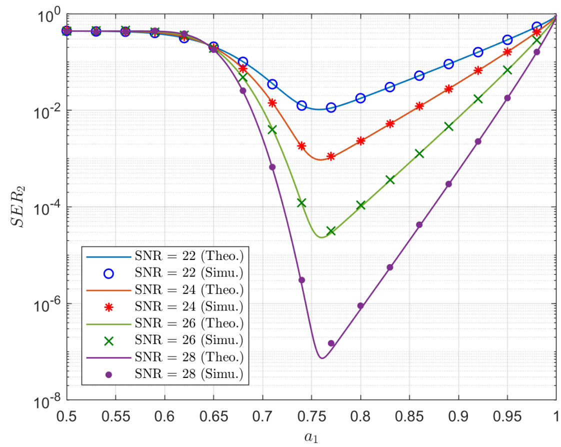

FIGURE 8. SER of the second user vs. the PA coefficient with various SNR values.

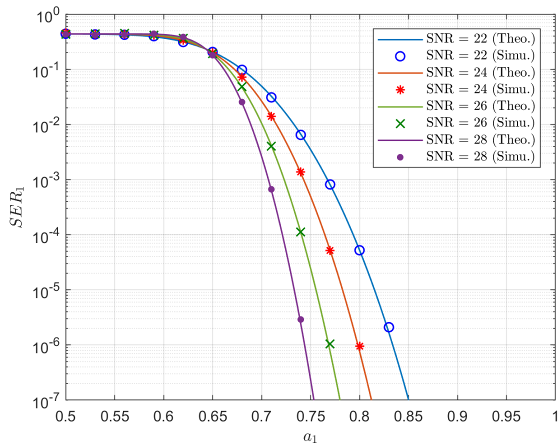

FIGURE 7. SER of the first user vs. the PA coefficient with various SNR values.

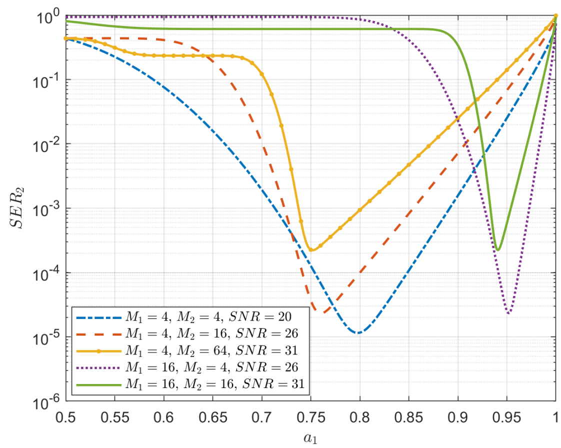

FIGURE 9. SER of the second user vs. the PA coefficient with various modulation schemes.

to the second user is decreased. Consequently, the AWGN effect on the signal of the second user increases. Therefore, SER_2 finally increases again.

Fig. 9 presents the SER of the second user for various modulation orders. The optimal PA, namely, the PA that minimizes SER_2, differs among the modulation schemes. Typically, in NOMA, the modulation order of the first user is smaller than the modulation order of the second user since the first user has poorer channel conditions. However, if the first-user SNR is sufficiently high, it is possible to use a greater modulation order if the second user does not require a higher data rate.

Table 1 summarizes the values of a_1 and a_2 that result in the first overlap in the superimposed constellation. The symbols start to overlap even if the condition $a_1 > a_2$ is satisfied. Hence, condition (59) for PA is not sufficient for a NOMA-based system with higher order modulation. Moreover, the PA depends on the modulation orders of the users. For example, if $M_1 = 4$, $M_2 = 4$ and the maximum allowed SER for the second user is 10^{-4}, the suitable PA condition (from Fig. 9) is $0.75 < a_1 < 0.85$. Then, according to the SNR for the first user, we can choose a suitable value of a_1 within this range. In contrast, if $M_1 = 4$, $M_2 = 16$ and the maximum allowed SER for the second user is 10^{-4}, which requires a higher SNR, the suitable PA condition (from Fig. 9) is $0.74 < a_1 < 0.8$.

TABLE 1. PA that causes the first overlap in the superimposed constellation for various modulation schemes.

First-user modulation	Second-user modulation	a_1	a_2
4-QAM	4-QAM	0.5	0.5
4-QAM	16-QAM	0.6429	0.3571
4-QAM	64-QAM	0.7	0.3
16-QAM	4-QAM	0.8333	0.1667
16-QAM	16-QAM	0.9	0.1

Table 2 summarizes the values of the PA coefficients that minimize the SER of the second user for various modulation orders. These PA coefficients are calculated via (68) and they agree with the optimal values of the PA coefficients in Fig. 9,

TABLE 2. Optimal PA for the second user.

s_1	s_2	x	a_1	a_2	d_{min}
BPSK	4-QAM	8-QAM	0.6667	0.3333	0.8165
4-QAM	4-QAM	16-QAM	0.8	0.2	0.6325
4-QAM	16-QAM	64-QAM	0.7619	0.2381	0.3086
4-QAM	64-QAM	256-QAM	0.7529	0.2471	0.1534
16-QAM	4-QAM	64-QAM	0.9524	0.0476	0.3086
16-QAM	16-QAM	256-QAM	0.9412	0.0588	0.1534

which supports the validity of the derived formulas. When $M_1 = 4$ and $M_2 = 16$, the superimposed constellation has the same number of symbols as when $M_1 = 16$ and $M_2 = 4$. However, the PA coefficients differ between the cases. This finding can be explained as follows: The constellation of the first user becomes denser, namely, the minimum distance decreases, as the modulation order of the first user increases. Hence, the addition of the noise and the interference from the second user will cause the first user to require a higher SNR, which corresponds to a higher PA coefficient.

VI. CONCLUSION

In this paper, a downlink NOMA-based VLC system with higher order modulation has been investigated. General and closed-form SER expressions have been derived in which the symbols of each user that are generated using any square M-QAM are considered. The derived expressions have been validated via computer simulation. A necessary and sufficient PA constraint has been proposed for practical NOMA-based systems with higher order modulation schemes for reducing the error in data detection. It has been shown that the PA depends on the modulation order of each user.

ACKNOWLEDGMENT

The authors would like to thank the Deanship of Scientific Research at King Saud University for supporting this research through the initiative of DSR Graduate Students Research Support (GSR).

REFERENCES

[1] H. Tullberg, P. Popovski, Z. Li, M. A. Uusitalo, A. Hoglund, O. Bulakci, M. Fallgren, and J. F. Monserrat, "The metis 5G system concept: Meeting the 5G requirements," *IEEE Commun. Mag.*, vol. 54, no. 12, pp. 132–139, Dec. 2016.

[2] L. Feng, R. Q. Hu, J. Wang, P. Xu, and Y. Qian, "Applying VLC in 5G networks: Architectures and key technologies," *IEEE Netw.*, vol. 30, no. 6, pp. 77–83, Nov./Dec. 2016.

[3] S. S. Bawazir, P. C. Sofotasios, S. Muhaidat, Y. Al-Hammadi, and G. K. Karagiannidis, "Multiple access for visible light communications: Research challenges and future trends," *IEEE Access*, vol. 6, pp. 26167–26174, 2018.

[4] L. Dai, B. Wang, Z. Ding, Z. Wang, S. Chen, and L. Hanzo, "A survey of non-orthogonal multiple access for 5G," *IEEE Commun. Surveys Tuts.*, vol. 20, no. 3, pp. 2294–2323, 3rd Quart., 2018.

[5] H. Marshoud, V. M. Kapinas, G. K. Karagiannidis, and S. Muhaidat, "Non-orthogonal multiple access for visible light communications," *IEEE Photon. Technol. Lett.*, vol. 28, no. 1, pp. 51–54, Jan. 1, 2016.

[6] J. Shi, J. He, K. Wu, and J. Ma, "Enhanced performance of asynchronous multi-cell vlc system using oqam/ofdm-noma," *J. Lightw. Technol.*, vol. 37, no. 20, pp. 5212–5220, Oct. 15, 2019.

[7] S. Dimitrov and H. Haas, *Principles LED Light Communications: Towards Networked Li-Fi*. Cambridge, U.K.: Cambridge Univ. Press, 2015.

[8] S. Dimitrov, S. Sinanovic, and H. Haas, "Signal shaping and modulation for optical wireless communication," *J. Lightw. Technol.*, vol. 30, no. 9, pp. 1319–1328, May 1, 2012.

[9] S. D. Dissanayake and J. Armstrong, "Comparison of ACO-OFDM, DCO-OFDM and ADO-OFDM in IM/DD systems," *J. Lightw. Technol.*, vol. 31, no. 7, pp. 1063–1072, Apr. 1, 2013.

[10] S. M. R. Islam, N. Avazov, O. A. Dobre, and K.-S. Kwak, "Power-domain non-orthogonal multiple access (NOMA) in 5G systems: Potentials and challenges," *IEEE Commun. Surveys Tuts.*, vol. 19, no. 2, pp. 721–742, 2nd Quart., 2017.

[11] H. Haas, L. Yin, Y. Wang, and C. Chen, "What is LiFi?" *J. Lightw. Technol.*, vol. 34, no. 6, pp. 1533–1544, Mar. 15, 2016.

[12] C. Chen, W. De Zhong, H. Yang, and P. Du, "On the performance of MIMO-NOMA-based visible light communication systems," *IEEE Photon. Technol. Lett.*, vol. 30, no. 4, pp. 307–310, Feb. 15, 2018.

[13] Y. Fu, Y. Hong, L. Chen, and C. W. Sung, "Enhanced Power Allocation for Sum Rate Maximization in OFDM-NOMA VLC Systems," *IEEE Photon. Technol. Lett.*, vol. 30, no. 13, pp. 1218–1221, Jul. 1, 2018.

[14] L. Yin, X. Wu, and H. Haas, "On the performance of non-orthogonal multiple access in visible light communication," in *Proc. IEEE 26th Annu Int. Symp. Pers., Indoor, Mobile Radio Commun. (PIMRC)*, Aug./Sep. 2015, pp. 1354–1359.

[15] L. Yin, W. O. Popoola, X. Wu, and H. Haas, "Performance evaluation of non-orthogonal multiple access in visible light communication," *IEEE Trans. Commun.*, vol. 64, no. 12, pp. 5162–5175, Dec. 2016.

[16] H. Ren, Z. Wang, S. Han, J. Chen, C. Yu, C. Xu, and J. Yu, "Performance improvement of M-QAM OFDM-NOMA visible light communication systems," in *Proc. IEEE Global Commun. Conf. (GLOBECOM)*, Dec. 2018, pp. 1–6.

[17] C. Chen, W. Zhong, H. Yang, P. Du, and Y. Yang, "Flexible-rate SIC-free NOMA for downlink VLC based on constellation partitioning coding," *IEEE Wireless Commun. Lett.*, vol. 8, no. 2, pp. 568–571, Apr. 2019.

[18] H. Li, Z. Huang, Y. Xiao, S. Zhan, and Y. Ji, "Solution for error propagation in a NOMA-based VLC network: Symmetric superposition coding," *Opt. Express*, vol. 25, no. 24, pp. 29856–29863, 2017. [Online]. Available: http://www.opticsexpress.org/abstract.cfm?URI=oe-25-24-29856

[19] H. Marshoud, P. C. Sofotasios, S. Muhaidat, G. K. Karagiannidis, and B. S. Sharif, "Error performance of NOMA VLC systems," in *Proc. IEEE Int. Conf. Commun. (ICC)*, May 2017, pp. 1–6.

[20] H. Marshoud, P. C. Sofotasios, S. Muhaidat, G. K. Karagiannidis, and B. S. Sharif, "On the performance of visible light communication systems with non-orthogonal multiple access," *IEEE Trans. Wireless Commun.*, vol. 16, no. 10, pp. 6350–6364, Oct. 2017.

[21] H. Huang, J. Wang, J. Wang, J. Yang, J. Xiong, and G. Gui, "Symbol error rate performance analysis of non- orthogonal multiple access for visible light communications," *China Commun.*, vol. 14, no. 12, pp. 153–161, Dec. 2017.

[22] X. Liu, Y. Wang, F. Zhouz, and R. Q. Hu, "Ber analysis for noma-enabled visible light communication systems with m-psk," in *Proc. 10th Int. Conf. Wireless Commun. Signal Process. (WCSP)*, Oct. 2018, pp. 1–7.

[23] L. Bariah, S. Muhaidat, and A. Al-Dweik, "Error probability analysis of non-orthogonal multiple access over Nakagami-*m* fading channels," *IEEE Trans. Commun.*, vol. 67, no. 2, pp. 1586–1599, Feb. 2019.

[24] T. Assaf, A. Al-Dweik, M. E. Moursi, and H. Zeineldin, "Exact ber performance analysis for downlink noma systems over nakagami-*m* fading channels," *IEEE Access*, vol. 7, pp. 134539–134555, 2019.

[25] J. G. Proakis and M. Salehi, *Digital communications*, vol. 4. New York, NY, USA: McGraw-Hill, 2001.

[26] E. Yoon, "Maximum likelihood detection with a closed-form solution for the square QAM constellation," *IEEE Commun. Lett.*, vol. 21, no. 4, pp. 829–832, Apr. 2017.

ESAM M. ALMOHIMMAH received the B.Sc. degree (Hons.) in electrical engineering from Sana'a University, Yemen, and the M.Sc. degree in electrical engineering from King Saud University, Riyadh, Saudi Arabia, where he is currently pursuing the Ph.D. degree with the Department of Electrical Engineering. His research interests include optical wireless communications, indoor visible light communication, and digital communication.

MOHAMMED T. ALRESHEEDI received the B.Sc. degree (Hons.) in electrical engineering from King Saud University, Riyadh, Saudi Arabia, in 2006, and the M.Sc. degree (Hons.) in communication engineering and the Ph.D. degree in electronic and electrical engineering from the University of Leeds, Leeds, U.K., in 2009 and 2014, respectively. He is currently an Associate Professor with the Department of Electrical Engineering, King Saud University. His research interests include adaptive techniques for optical wireless (OW), OW systems design, indoor OW networking, and visible light communications.